Optica Applicata, Vol. XL, No. 1, 2010

Continuous wave terahertz spectrometer based on two DFB laser diodes

RAFAŁ WILK

Institute for High-Frequency Technology, Schleinitzstrasse 22, 32106 Braunschweig, Germany;
e-mail: r.wilk@menlosystems.com

Menlo Systems GmbH, Am Klopferspitz 19, 82152 Martinsried, Germany

In this paper, a continuous wave (cw) spectrometer in the far infrared range is presented. Electromagnetic radiation is generated via photomixing phenomena and covers frequencies between about 50 GHz and 1.1 THz with resolution of about 10 GHz. The measured emission characteristics of different antenna types are compared to simulation results. Transmission measurements of Bragg structure for terahertz frequencies proved high spectral resolution of the spectrometer.

Keywords: terahertz, continuous wave spectroscopy, Bragg structure.

1. Introduction

Terahertz technology is related to a frequency range between several tens of gigahertz up to several terahertz (wave numbers between about 2 cm^{-1} and 200 cm^{-1}). This frequency range located between those covered by optical technology and high speed electronics is still relatively unexplored. Despite a multitude of applications [1–4], which are discussed for this frequency window, the THz technology is still underdeveloped and cost-effective systems are still lacking.

High speed microwave and electronics components can only cover the lower THz range. In connection with mixers and multipliers, state-of-the-art microwave diodes can generate frequencies up to 1 THz. High-speed microwave components are relatively expensive and are not tuneable over broad frequency range [5]. On the other hand, far infrared gas lasers [6] or semiconductor quantum cascade lasers (QCLs) operate in the upper THz range [7]. Gas lasers are bulky and can emit several mW of power only at discrete THz frequencies. QCLs are compact sources, but require cryogenic cooling. The most powerful THz generation approach in terms of cost, size and tuneability is represented by photoconductive antennas which are gated by ultrashort laser pulses to generate broad-band THz pulses (THz time-domain spectroscopy, TDS) [8, 9]. Yet, these state of the art THz spectrometers rely on

femtosecond lasers as a core component. Alternatively, one can use two independent diode lasers the emission of which is superimposed onto the THz antenna. In this case the antenna emits tunable cw THz waves. This approach is called photomixing and is somewhat less explored [10–13] than TDS. State-of-the-art photomixing systems with laser diodes stabilized to Fabry–Pérot etalon can archive a frequency resolution on the 1 MHz level [14]. Most of the cw spectrometers reported so far were based on very fragile antennas with interdigitated structures in the excitation gap.

In this paper a simple continuous wave THz spectrometer is presented. The spectrometer is based on two DFB diodes, low temperature grown gallium arsenide (LT-GaAs) photomixer antenna with simple excitation gap and bolometr detector.

2. Generation and detection of cw THz waves

In the following section, a process of optical heterodyne conversion, often referred to as photomixing, is described. The mixing process of two waves with slightly different frequencies f_1 and f_2 leads to a beating, as shown in Fig. 1. Such a mixing of two acoustic waves is very well known in our daily life. Here, this phenomenon of mixing of two optical beams with wavelengths λ_1 and λ_2 is utilized for generation of electromagnetic waves with gigahertz and terahertz frequencies.

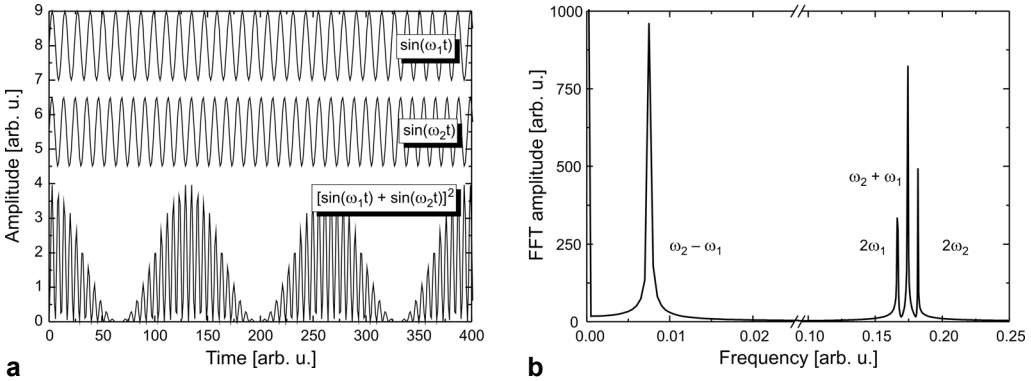

Fig. 1. Interference of two optical waves in time domain (**a**) and FFT spectrum (**b**).

For simplicity it is assumed that the amplitudes of their electric fields E_0 are equal, beams are collinear polarized and they overlap completely.

When the two optical beams interfere with each other on a photomixer, which is typically LT-GaAs, the resulting electric field $E(t)$ and incident optical power $P_i(t)$ are equal to:

$$E(t) = E_0\cos(\omega_1 t) + E_0\cos(\omega_2 t) = 2E_0\cos\left(\frac{\omega_1 + \omega_2}{2}t\right)\cos\left(\frac{\omega_1 - \omega_2}{2}t\right) \tag{1}$$

$$P_i(t) \propto E^2(t) =$$

$$= E_0^2\left[1 + \cos(\omega_1 + \omega_2)t + \cos(\omega_1 - \omega_2)t + \frac{1}{2}\cos(2\omega_1 t) + \frac{1}{2}\cos(2\omega_2 t)\right] \tag{2}$$

The product of the mixing process are four waves with frequencies $f_1 - f_2$, $2f_1$, $2f_2$ and $f_1 + f_2$. The $2f_1$, $2f_2$ and $f_1 + f_2$ components oscillate on a much faster time scale (*ca*. 700 THz) than electron–hole recombination time τ in a photomixer and therefore can be neglected. The optical beating periodically modulates the photoconductance of the antenna deposited on the LT-GaAs. Under the presence of external electric field (bias) in addition to DC photocurrent, an $f_1 - f_2$ AC component will be flowing through the antenna and thus radiate EM wave.

Power of radiated THz electromagnetical wave is proportional to the square of incident optical power P_i and square of applied bias to the antenna V_B:

$$P_{\mathrm{THz}} \propto P_i^2 V_B^2 k \tag{3}$$

where k is a factor depending on the antenna structure, radiation efficiency and carrier dynamics in the LT-grown layer. The most accurate models of the photomixing mechanism for the generation of THz waves were developed by Brown *et al*. [15] and Saeedkia *et al.* [16].

THz photon energy of 1.24 meV at 0.3 THz is well below values acceptable for photodiodes based detectors widely used in the visible and infrared range. Therefore, the most commonly used detectors for the THz range are based on thermal effects and include bolometers, Golay cells and pyrodetectors. The basic element of thermal detectors is a low heat capacity absorber which is heated up under illumination of incident radiation. Such thermal detectors are responsive over a very broad wavelength range stretching from microwaves to the infrared. The bolometer is capable of measuring very weak THz signals in the range of nW. Typically, the detection speed of thermal detectors is limited to about 10 to 25 Hz.

3. Experimental setup

Figure 2 shows the experimental setup. Optical beams from two DFB GaAs/AlGaAs laser diodes are combined by 50:50 beamsplitter cube. The emission wavelength of the diodes can be tuned between 857.9 nm and 861.3 nm by changing the temperature of the diode from 1 °C to 50 °C, respectively. Therefore, the maximal difference frequency between the two diodes equals to 1.38 THz.

The two-colour beam with an integrated optical power of 35 mW is guided and focused onto a photomixer. The antenna is biased with 40 V copped at 20 Hz. The terahertz radiation emitted by the photoconductive dipole antenna is pre-collimated with a high-resistivity Si-lens of hypersemispherical shape [17, 18]. The THz beam is

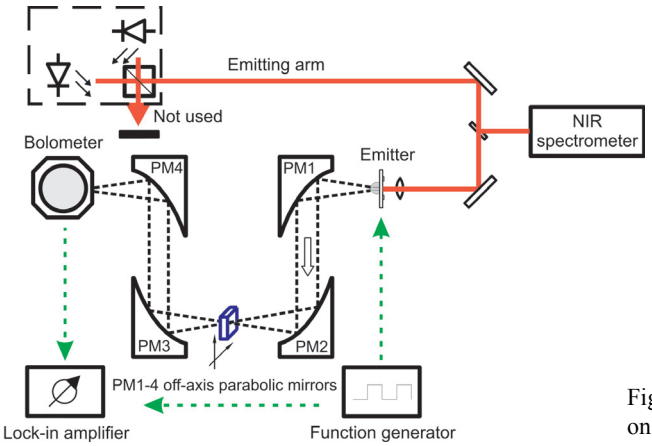

Fig. 2. Cw terahertz spectrometer based on thermal detection.

guided via four off-axis parabolic mirrors (PM) PM1–PM4 to the bolometer working as THz detector. Between the PM2 and PM3 mirrors an intermediate focus is formed, where the sample under investigation can be placed. Finally, THz radiation is guided to the bolometer detector. The transmitting antenna is chopped electrically with a unipolar square waveform between on and off state. The signal from the bolometer is measured with a lock-in amplifier. Laser emission wavelengths are monitored by a low-cost near infrared (NIR) spectrometer. Its spectral resolution of about 0.5 nm determines the 10 GHz frequency step of measurements in THz range, as given by:

$$f_{\mathrm{THz}} = f_1 - f_2 = \frac{c}{\lambda_1} - \frac{c}{\lambda_2} \tag{4}$$

where c is speed of light, λ and f are wavelengths and corresponding frequencies of the laser beams.

3.1. Photomixer and THz antenna structure

The typical photomixer for excitation with wavelengths shorter than 860 nm is based on low-temperature (LT) grown GaAs. This 2 μm thick LT layer grown at 300 °C on a semi-insulating (SI) GaAs is characterized with sub-ps carrier lifetime and thus is capable of response in THz range. On the top of the epitaxial layer, a planar metal structure of the THz antenna is deposited, using the standard lift-off technique.

There are several possible shapes of THz antennas. The most common ones are narrow-band dipoles or somewhat less efficient broad-band antennas, like bow-ties or spiral-log antennas. Because photomixing efficiency is in general low, typically, highly efficient, but very fragile antennas with interdigitated (finger) structures in the excitation gap are used. In this paper all presented results are based on simple and robust dipole antennas. The antenna structure is shown in Fig. 3. The dipole structure of a length L_{dipole} is located in the central part of the chip between two long striplines for applying the bias. The striplines are terminated by four 1 mm × 1 mm contact pads. Dipole antennas used in the presented experimental setup comprise dipoles with

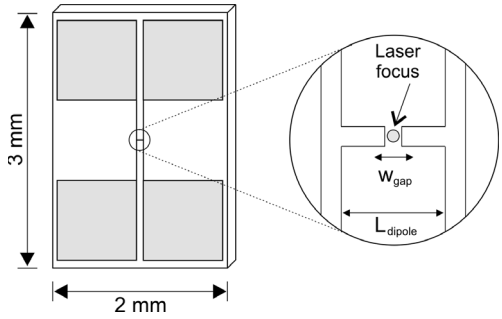

Fig. 3. THz photomixer.

a length of L_{dipole} = 200 μm and L_{dipole} = 100 μm. A two-color laser beam is focused in an excitation gap with a width of w_{gap} = 5 μm which is located in the middle of each dipole structure, as shown in Fig. 3. The incident optical power is limited to 35 mW due to damage threshold of a photomixer. The obtained photocurrent is in a range of 300 μA for both photomixers.

3.2. Experimental results

The Si-bolometer used as a THz detector has a flat spectral characteristic and allows direct measurement of the emission spectra of photomixer antennas.

In the first experiment, emission spectra of antennas with 200 μm and 100 μm dipoles were investigated. The emission of the first laser diode was set to 857.8 nm. The wavelength f_0 of the second diode was swept between 857.9 nm and 860.5 nm. Therefore, a spectrum between about 50 GHz and 1100 GHz was covered. Figures 4**b** and 4**c** show the measured antennas emission characteristics together with simulation results. Theoretical spectra were calculated in a commercially available software [19]. The simulated antennae correspond to the real-life structures, as shown in Fig. 3. For simplicity, it was assumed that the antenna structure deposited on the GaAs is made of perfect conductor. The attached Si-lens was assumed to be half-space. The calculated S_{12} parameters normalized to the measured spectra are shown in Fig. 4. Both, the calculated and measured spectra agree reasonably well. The spectrum of 200 μm dipole exhibits two broad resonances around 200 GHz and 700 GHz corresponding to the fundamental resonance and its third harmonics, respectively. One can easily observe that the measured and simulated spectra are of rippled shape and comprise several narrow-band sub-resonances, especially at frequencies below 400 GHz. This fact is contributed to the finite chip size which is comparable with the emission wavelength at the lower frequency range. Therefore, the antenna cannot be considered as a perfect dipole. The third harmonic resonance is already ripple-free. One can observe small dips in the measured spectrum at 550 GHz and 750 GHz, which originate from water-vapor absorption lines [20]. The second investigated antenna with 100 μm dipole has one broad resonance around 400 GHz. Again, the spectrum showed in Fig. 4**c** exhibits several ripples at low frequencies, whereas the high frequency part of the spectrum is more uniform. SNR of both measurements is in the range of 35–40 dB.

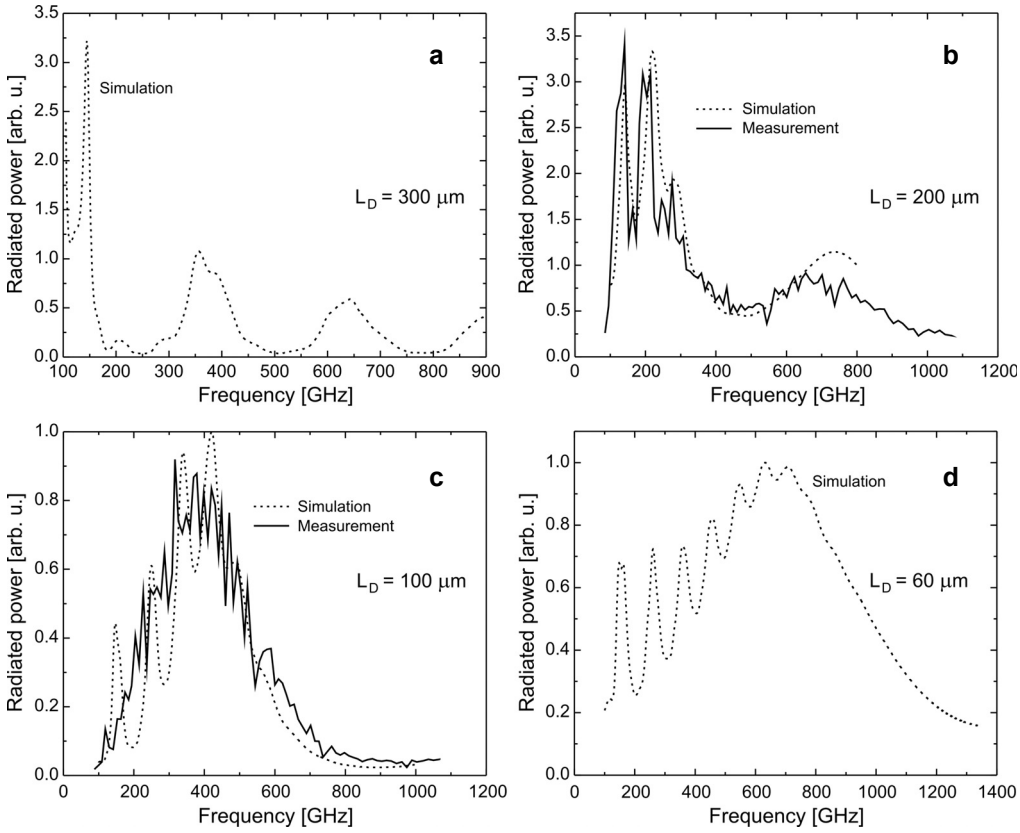

Fig. 4. The simulated and measured spectrum of 300 μm (**a**), 200 μm (**b**), 100 μm (**c**) and 60 μm (**d**) dipole antennas.

In addition to the investigated antennas, Figs. 4**a** and 4**d** show the simulated emission spectrum of antennas with 300 μm and 60 μm dipole, respectively. The 300 μm dipole has a low frequency resonance around 100 GHz and higher order harmonics around 0.35 THz, 0.65 THz and 0.9 THz. The simulation of 60 μm shows very broad resonance around 700 GHz. In general, with an increase in frequency high order resonances get smaller in amplitude. This is contributed to the nature of the antenna and to the lower mixing efficiency at higher frequencies [15]. With a decrease in the dipole length, the antenna's natural resonance shifts towards higher frequencies. Moreover, high frequency resonances are considerably broader than resonances at lower frequency range.

To demonstrate the spectroscopic capability of the system, a measurement of the Bragg structure for THz frequencies was performed. The test sample is a manually stapled multilayer structure composed of polypropylene (PP) foils and silicon (Si) slices. Four 63 μm thick layers of high resistivity silicon with a refractive index of 3.418 are sandwiched between five 150 μm thick layers of polypropylene foil with a refractive index of 1.530. The simulated transmission spectrum of the Bragg

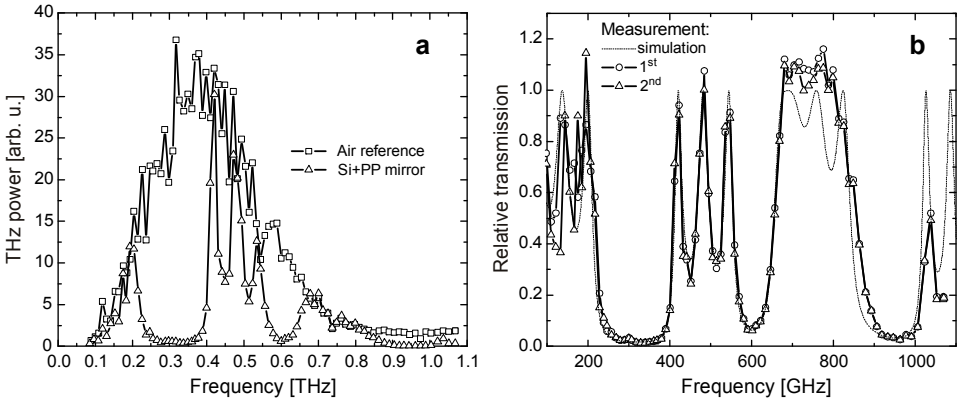

Fig. 5. The measured transmission spectrum of Bragg structure for THz frequencies.

structure is shown in Fig. 5**b**. Calculations were based on a commonly used transfer matrix method [21]. The Bragg structure is designed to exhibit a broad stop-band (reflection band) between 240 GHz and 370 GHz. Moreover, the structure has a couple of very sharp figures and therefore acts as a perfect test sample for system evaluation. More details about the tested Bragg structure and measurements performed in the time-domain spectrometer can be found in [22]. Figure 5**a** shows the measured reference signal and the one transmitted through the mirror. The measured signals contain number of irregular features and may look noisy. However, the excellent reproducibility between the two measurements showed in Fig. 5**b** proves that the irregularities originate not from noise, but from the antenna's emission characteristics. The measurements disagree somewhat at lower frequencies due to the limited resolution of the low-cost near infrared spectrometer used in the setup. At low frequencies, both laser lines partially overlap and determination of THz frequencies is difficult. For frequencies above 150 GHz, the experimentally measured and simulated transmission spectra agree very well with each other.

4. Conclusions

In this paper, a continuous wave far infrared spectrometer covering electromagnetic spectrum between about 50 GHz and 1.1 THz is presented. THz radiation is generated via photomixing phenomena of two beams from DFB laser diodes. Emission spectra of 100 μm and 200 μm LT-GaAs dipole antennas used in the spectrometer were measured using a bolometer detector. Transmission measurements of the test Bragg structure for THz frequencies proved very good resolution of the spectrometer.

References

[1] PIESIEWICZ R., KLEINE-OSTMANN T., KRUMBHOLZ N., MITTLEMAN D., KOCH M., SCHOEBEL J., KURNER T., *Short-range ultra-broadband terahertz communications: Concepts and perspectives*, IEEE Antennas and Propagation Magazine **49**(6), 2007, pp. 24–39.

[2] FISCHER B., HOFFMANN M., HELM H., WILK R., RUTZ F., KLEINE-OSTMANN T., KOCH M., JEPSEN P., *Terahertz time-domain spectroscopy and imaging of artificial RNA*, Optics Express **13**(14), 2005, pp. 5205–5215.
[3] FEDERICI J.F., SCHULKIN B., HUANG F., GARY D., BARAT R., OLIVEIRA F., ZIMDARS D., *THz imaging and sensing for security applications – explosives, weapons and drugs*, Semiconductor Science and Technology **20**(7), 2005, pp. S266–S280.
[4] KRUMBHOLZ N., HOCHREIN T., VIEWEG N., HASEK T., KRETSCHMER K., BASTIAN M., MIKULICS M., KOCH M., *Monitoring polymeric compounding processes inline with THz time-domain spectroscopy*, Polymer Testing **28**(1), 2009, pp. 30–35.
[5] CHATTOPADHYAY G., SCHLECHT E., WARD J. S., GILL J.J., JAVADI H.H.S., MAIWALD F., MEHDI I., *An all-solid-state broad-band frequency multiplier chain at 1500 GHz*, IEEE Transactions on Microwave Theory and Techniques **52**(5), 2004, pp. 1538–1547.
[6] ABRAMSKI K.M., PLINSKI E.F., *Other gas lasers*, [In] *Gas Lasers*, [Eds.] M. Endo, R.F. Walter, CRC Press, New York, 2007, pp. 497–539.
[7] FAIST J., CAPASSO F. , SIVCO D. L. , SIRTORI C., HUTCHINSON A.L., CHO A.Y., *Quantum cascade laser*, Science **264**(5158), 1994, pp. 553–556.
[8] GRISCHKOWSKY D., KEIDING S., VAN EXTER M., FATTINGER CH., *Far-infrared time-domain spectroscopy with terahertz beams of dielectrics and semiconductors*, Journal of the Optical Society of America B **7**(10), 1990, pp. 2006–2015.
[9] SARTORIUS B., ROEHLE H., KÜNZEL H., BÖTTCHER J., SCHLAK M., STANZE D., VENGHAUS H., SCHELL M., *All-fiber terahertz time-domain spectrometer operating at 1.5 μm telecom wavelengths*, Optics Express **16**(13), 2008, pp. 9565–9570.
[10] BROWN E.R., MCINTOSH K.A., NICHOLS K.B., DENNIS C.L., *Photomixing up to 3.8 THz in low-temperature-grown GaAs*, Applied Physics Letters **66**(3), 1995, pp. 285–287.
[11] MATSUURA S., TANI M., SAKAI K., *Generation of coherent terahertz radiation by photomixing in dipole photoconductive antennas*, Applied Physics Letters **70**(5), 1997, pp. 559–561.
[12] BIGOURD D., CUISSET A., HINDLE F., MATTON S., FERTEIN E., BOCQUET R., MOURET G., *Detection and quantification of multiple molecular species in mainstream cigarette smoke by continuous-wave terahertz spectroscopy*, Optics Letters **31**(15), 2006, pp. 2356–2358.
[13] GREGORY I.S., TRIBE W.R., BAKER C., COLE B.E., EVANS M.J., SPENCER L., PEPPER M., MISSOUS M., *Continuous-wave terahertz system with a 60 dB dynamic range*, Applied Physics Letters **86**(20), 2005, p. 204104.
[14] DENINGER A.J., GÖBEL T., SCHÖNHERR D., KINDER T., ROGGENBUCK A., KÖBERLE M., LISON F., MÜLLER-WIRTS T., MEISSNER P., *Precisely tunable continuous-wave terahertz source with interferometric frequency control*, Review of Scientific Instruments **79**(4), 2008, p. 044702.
[15] BROWN E.R., SMITH F.W., MCINTOSH K.A., *Coherent millimeter-wave generation by heterodyne conversion in low-temperature-grown GaAs photoconductors*, Journal of Applied Physics **73**(3), 1993, pp. 1480–1484.
[16] SAEEDKIA D., MANSOUR R.R., SAFAVI-NAEINI S., *The interaction of laser and photoconductor in a continuous-wave terahertz photomixer*, IEEE Journal of Quantum Electronics **41**(9), 2005, pp. 1188–1196.
[17] JEPSEN P., JACOBSEN R.H., KEIDING S.R., *Generation and detection of terahertz pulses from biased semiconductor antennas*, Journal of the Optical Society of America B **13**(11), 1996, pp. 2424–2436.
[18] VAN RUDD J., MITTLEMAN D.M., *Influence of substrate-lens design in terahertz time-domain spectroscopy*, Journal of the Optical Society of America B **19**(2), 2002, pp. 319–329.
[19] CST Microwave Studio.
[20] VAN EXTER M., FATTINGER CH., GRISCHKOWSKY D., *Terahertz time-domain spectroscopy of water vapor*, Optics Letters **14**(20), 1989, pp. 1128–1130.

[21] BORN M., WOLF E., *Principles of Optics*, 6th Ed., Pergamon Press, 1994.
[22] KRUMBHOLZ N., GERLACH K., RUTZ F., KOCH M., PIESIEWICZ R., KÜRNER T., MITTLEMAN D., *Omnidirectional terahertz mirrors: A key element for future terahertz communication systems*, Applied Physics Letters **88**(20), 2006, p. 202905.

Received May 15, 2009
in revised form July 29, 2009